

G. MÉJEAN
J. KASPIAN
J. YU
S. FREY
E. SALMON
J.-P. WOLF[✉]

Remote detection and identification of biological aerosols using a femtosecond terawatt lidar system

Teramobile Project, LASIM, UMR CNRS 5579, Université Claude Bernard Lyon 1, 43 bd. du 11 Novembre 1918, 69622 Villeurbanne Cedex, France

Received: 30 January 2004

Published online: 24 February 2004 • © Springer-Verlag 2004

ABSTRACT We demonstrate experimentally the first range-resolved detection and identification of biological aerosols in the air by non-linear lidar. Ultra-short terawatt laser pulses are used to induce two-photon-excited fluorescence (2PEF) in riboflavin-containing particles at a remote location. We show that, in the case of amino acid detection, 2PEF-lidar should be more efficient than linear 1PEF-lidar beyond a typical distance of 2 km, because it takes advantage of the higher atmospheric transmission at the excitation wavelengths. 2PEF-lidar moreover allows size measurement by pump-probe schemes, and pulse shaping may improve the detection selectivity.

PACS 33.50.-j; 33.80.Wz; 42.65.-k; 42.68.Wt; 92.60.Mt

The early detection and identification of potentially harmful bioagents in the air has become a major issue for both defence and public security reasons. This requires fast detection of the outbreak location, 3D mapping of the plume as it propagates, and unambiguous identification of the agents among the broad variety of atmospheric background aerosols. In this letter, we study the application of fluorescence-based lidar (light detection and ranging) [1] towards these goals. We demonstrate experimentally the first remote detection and identification of bioagent simulants (riboflavin-doped microparticles) in the air by non-linear lidar. We used ultra-short laser pulses from the Teramobile [2, 3] to induce in situ two-photon-excited fluorescence (2PEF) [4] in the aerosol particles. Two major reasons motivate the use of ultra-short multiphoton excitation: (1) the better atmospheric transmission at longer wavelengths (decrease of Rayleigh scattering and prevention of molecular absorption such as ozone) and (2) the possibility of simultaneous size measurement by pump-probe schemes [5, 6] and coher-

ent excitation with shaped pulses [7, 8] to improve the detection selectivity.

Most of the bioagents, like the bacillus anthracis (anthrax), are bacteria of typically 1 μm in size [9]. Depending on the spread conditions, they can agglomerate in clusters of sizes up to 10 μm . They contain natural fluorophores, like amino acids (e.g. tryptophan), nicotine amides (NADH), and flavins (e.g. riboflavin (RBF) and flavoproteins), which can be used as characteristic tracers of their biological nature [10]. We used the specific fluorescence signature at 540 nm of riboflavin, which we excited with two photons at the fundamental wavelength (800 nm) of the first terawatt lidar system, the Teramobile [2, 3]. The Teramobile is based on a chirped pulse amplified (CPA) laser that delivers 5-TW pulses (80 fs, 400 mJ) at a 10-Hz repetition rate. The laser pulses are sent into the atmosphere using an all-reflective beam expander. The backward-emitted fluorescence and scattered signals are collected by a 40-cm or 20-cm telescope depending on the application (longer or shorter distance measurements), which focuses

the light on a spectrally resolved detector. The returns are recorded as a function of the photons' flight time, providing distance resolution.

The bioagent simulants were produced with an aerosol generator located at 45 m from the Teramobile. Their size distribution and concentrations were monitored using an optical sizer (Grimm model G 1-108). They consisted of water droplets of 1- μm size on average containing 0.02 g/l riboflavin.

A key parameter to efficiently excite 2PEF in the microparticles is the control of the laser pulse intensity at the target location, because of the non-linear nature of the excitation process. For this, the pulses were shaped using a negative linear chirp (shorter wavelengths of the 20-nm broad laser spectrum are launched before the longer wavelengths) in order to compensate the air group-velocity dispersion (GVD) and reduce the initial pulse peak intensity to prevent early filamentation. The best negative chirp value, which corresponds to a 1-ps pulse, leads to the results shown in Fig. 1a. The corresponding intensity on the target is 10^{11} W/cm^2 . The detected 2PEF spectrum clearly identifies the presence of riboflavin-containing particles, and the lidar range resolution (via the measurement of the flight time of the light) allows the precise spatial localization of the biological aerosol plume. The plume is measured to be spread over some 10 m. The spatial resolution is 45 cm, limited by the fluorescence lifetime of 3 ns for this transition [11]. Notice that the contrast against fluorescence of the background aerosols present in the air at the time of the measurement is excellent. The 2PEF signature of riboflavin was compared to the spectrum from pure wa-

✉ Fax: +33-4724/45871, E-mail: wolf@lasim.univ-lyon1.fr

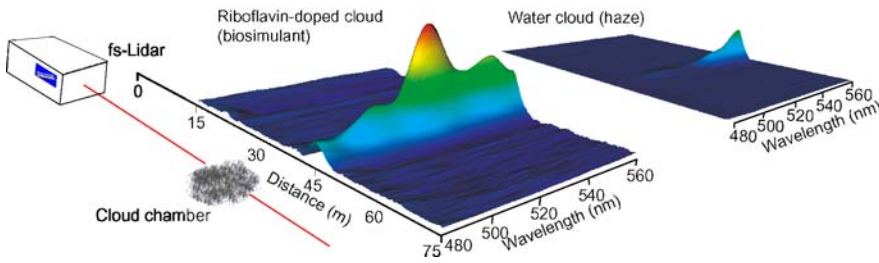


FIGURE 1 Remote detection and identification of bioaerosols. The femtosecond laser illuminates a plume of riboflavin (RBF)-containing microparticles 45-m away (left). The backward-emitted two-photon-excited fluorescence (2PEF), recorded as a function of distance and wavelength, exhibits the specific RBF fluorescence signature for the bioaerosols (middle) but not for pure water droplets (simulating haze, right)

ter microdroplets (Fig. 1b). This clearly demonstrates the capability of identifying biological particles from background non-biological ones of the same size. A smooth increase of the backscattered signal is observed over 600 nm for both bioagent simulants and pure water due to self-phase modulation (SPM) of the pulse as it propagates in air to the target. The spectrally broadened pulse is elastically scattered by the aerosol particles in the plume. If filamentation was not controlled using a negative chirp, the SPM broadening would extend towards UV-blue, which could partially mask the fluorescence signature of the bioparticles. These experiments also show that the one photon per pulse detection limit corresponds to a concentration as low as 10 particles per cubic centimeter, for a 10-m spatial resolution.

Using shorter-wavelength excitation (around 530 nm) would provide significant advantages as compared to the 800-nm wavelength: (1) the already high sensitivity would be further enhanced by using 2PEF from the amino acid tryptophan (Trp) [9, 10], the concentration of which is typically 10^4 times higher than riboflavin in bacteria (10^8 Trp molecules in a 1- μm particle [11]) and (2) two photons at 530 nm would not only excite tryptophan, but also NADH and riboflavin, whose fluorescence features around 320–370 nm, 420–500 nm, and 520–620 nm, respectively, would provide multiple cross-checking biological signatures of the particle [10].

We performed numerical simulations to estimate the performance of a non-linear 2PEF-lidar, compared to a linear 1PEF-lidar (emission wavelength 266 nm), in the case of tryptophan fluorescence detection. Although ultra-short terawatt lasers that emit

around 530 nm are not commercially available yet, recent developments in ytterbium-based lasers are very encouraging, reaching up to the petawatt level (at the fundamental wavelength, to be frequency doubled) in the laboratory. In these simulations, we assumed that the laser intensity decreases only by linear extinction processes (Rayleigh–Mie scattering and absorption from atmospheric molecules) as it propagates in air to the aerosol plume. The number $N_f(R)$ of n -photon-excited fluorescence (n PEF, $n = 1$ or 2 in the calculations below) photons/pulse detected from the distance R can be described by the following equation:

$$N_f(R) = \varrho(R) \sigma^{(n)} \eta I_0^n \tau \zeta(R, \lambda) \frac{A}{4\pi R^2} \times S \Delta R \exp \left(- \int_0^R \alpha(R, \lambda_f) - n\alpha(R, \lambda_p) dR \right),$$

where $\varrho(R)$ is the concentration of aerosol particles, $\sigma^{(n)}$ is the n -photon absorption cross section for one mi-

croparticle, η is the fluorescence yield, I_0 is the initial laser pulse intensity, τ is the pulse duration, A is the receiver telescope area, ζ is the detection efficiency, S is the beam surface, ΔR is the spatial resolution, and α is the atmospheric extinction at the fluorescence and excitation wavelengths λ_f and λ_p , respectively. α widely favors longer wavelengths, because of the λ^{-4} dependence of Rayleigh scattering and molecular absorption in the UV. Around 266 nm, the major absorbing molecule in the atmosphere is ozone.

In the simulations, we used the following parameters: particle size 1 μm (average diameter), 10^8 Trp molecules/particle, $\sigma^{(1)} = 2 \times 10^{-17} \text{ cm}^2$ [11], $\sigma^{(2)} = 1 \times 10^{-50} \text{ cm}^4 \text{ s/photon}$ [12, 13], $\eta = 0.13$ [11, 12], $\zeta = 0.2$, $A = 0.125 \text{ m}^2$ (40-cm-diameter telescope), and $S = 10 \text{ cm}^2$. The 1PEF-lidar simulations used the specifications of best commercially available Nd:Yag lasers (fourth harmonic), with 100 mJ at 266 nm and 10-ns pulse duration, while for the 2PEF simulations we used the Teramobile laser specifications (400 mJ, 80 fs). The cross sections are $\alpha_{1P} = \alpha_{\text{Rayleigh}}(266 \text{ nm}) + N_{\text{Ozone}} \sigma_{\text{Ozone}}(266 \text{ nm}) = 1.6 \times 10^{-4} \text{ m}^{-1} + N_{\text{Ozone}} \sigma_{\text{Ozone}}(266 \text{ nm})$ with $\sigma_{\text{Ozone}}(266 \text{ nm}) = 1 \times 10^{-17} \text{ cm}^2$, $\alpha_{2P} = \alpha_{\text{Rayleigh}}(530 \text{ nm}) = 1 \times 10^{-5} \text{ m}^{-1}$ (for atmospheric transmission parameters see [14]). Figure 2 shows the results of our simulations ($N_f(R)$ /pulse from Trp, for 1PEF- and 2PEF-lidars in the case of a 10-m-diameter plume containing 100 bacteria/ cm^3), as a function of the distance R between the plume and the lidar system. The ozone concentration of $50 \mu\text{g}/\text{m}^3$ (full line) is typical for populated areas (urban or peri-urban conditions). Because of the strong UV extinction, 2PEF-lidar is

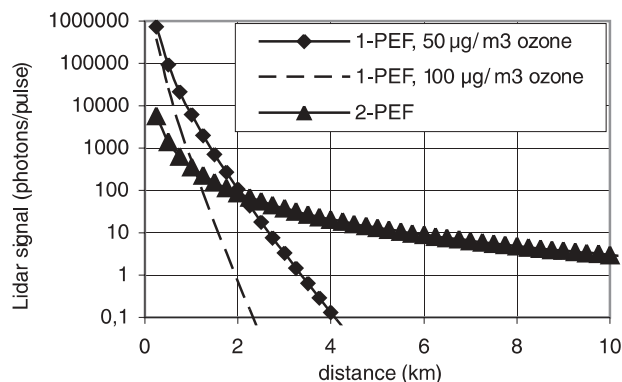


FIGURE 2 Simulated fluorescence lidar signal for tryptophan detection in bioaerosols. The collected 2PEF intensity is higher than 1PEF for distances over 1–2 km, due to the lower atmospheric transmission in the UV (Rayleigh scattering and ozone absorption, here typically 50 and 100 $\mu\text{g}/\text{m}^3$)

much more efficient than 1PEF-lidar for distances beyond 2 km. The distance R_0 beyond which 2PEF is more efficient than 1PEF strongly depends on the ozone concentration. In particular, 1PEF-lidar will not be practicable (limited to only a few hundred meters) in urban conditions in summer, where average O_3 concentrations very often exceed $100 \mu\text{g}/\text{m}^3$ (dashed line in Fig. 2; in ozone episodes up to $360 \mu\text{g}/\text{m}^3$, corresponding to the CEE 99 standard alarm level).

The simulations also provide estimations of the typical 2PEF-lidar detection limits. As $N_f(R)$ is proportional to the product $\rho(R)\Delta R$, the longer the integration distance, the better the sensitivity. As an example, for the average ozone concentration of $50 \mu\text{g}/\text{m}^3$, we obtain a minimum detectable concentration (corresponding to one fluorescence photon/pulse) as low as four bacteria/ cm^3 at 3 km or 10 bacteria/ cm^3 at 4 km with a 10-m distance resolution. At these distances and ozone concentrations, 1PEF-lidar detection is almost useless. Saturation and bleaching [12] do not affect these remarkable 2PEF-lidar sensitivities, as each two-photon-excited Trp molecule only emits typically 0.1 photon per exciting cycle. The estimated detection limit might strongly vary from one type of bacteria to another, because of the variations of the fluorescence quantum yield η [13]. Even for the values taken here [11], which correspond to fluorescence measurements of *bacillus subtilis* and *bacillus cereus*, variations of up to an order of magnitude have been observed. These varia-

tions in η , however, affect the absolute detection limits for a type of bacteria, but not the 1PEF- or 2PEF-lidar comparison.

The main limitation of 2PEF-lidar is, however, the ability to deliver the required intensity at the target plume location. In our simulations, we assumed the optimum situation where a successful control of the non-linear propagation (Kerr focusing and pulse compression) in air until the target was realized by using both spectral and spatial phase control. Although phase control could be demonstrated on distances in the 100-m range [3], and chirp-induced effects could be observed on self-phase modulation up to 10 km [2], no systematic investigation could be performed so far on the evolution of the beam intensity profile on the km scale. Further investigations, both theoretical and experimental, are therefore needed to better control the propagation of the ultrashort pulses to the target location. Sophisticated shaping techniques that allow us to precisely set the spectral and spatial phases of the laser pulse (temporal shaping and adaptive optics) will be of great use, as demonstrated for fusion applications [15]. Shaping the pulses in 2PEF experiments and using genetic algorithms moreover recently showed that two species exhibiting the identical linear fluorescence spectrum [7] can be efficiently distinguished. This remarkable experiment opens new perspectives in identifying bioagents from other fluorescing particles using 2PEF-lidars.

ACKNOWLEDGEMENTS Teramobile is a French–German project jointly funded by

the CNRS and the DFG. The authors wish to thank Steven C. Hill at ARL, Adelphi (MD) for very fruitful discussions, Marc Néri for helpful technical support, and Matthieu Jomier for assistance in preparing Fig. 1.

REFERENCES

- 1 J.-P. Wolf: in *Encyclopedia of Analytical Chemistry*, ed. by R.A. Meyers (Wiley, Chichester 2000) pp. 2226–2245
- 2 J. Kasparian, M. Rodriguez, G. Méjean, J. Yu, E. Salmon, H. Wille, R. Bourayou, S. Frey, Y.B. Andre, A. Mysyrowicz, R. Sauerbrey, J.P. Wolf, L. Woeste: *Science* **301**, 61 (2003)
- 3 H. Wille, M. Rodriguez, J. Kasparian, D. Mondelain, J. Yu, A. Mysyrowicz, R. Sauerbrey, J.P. Wolf, L. Woeste: *Eur. Phys. J. D* **20**, 183 (2002)
- 4 S.C. Hill, V. Boutou, J. Yu, S. Ramstein, J.P. Wolf, Y. Pan, S. Holler, R.K. Chang: *Phys. Rev. Lett.* **85**, 54 (2000)
- 5 J.P. Wolf, Y. Pan, S. Holler, G.M. Turner, M.C. Beard, R.K. Chang, A. Schmuttenmaer: *Phys. Rev. A* **64**, 023 808-1 (2001)
- 6 L. Méès, J.P. Wolf, G. Gouesbet, G. Gréhan: *Opt. Commun.* **208**, 371 (2002)
- 7 T. Brixner, N. Damrauer, P. Niklaus, G. Gerber: *Nature* **414**, 57 (2001)
- 8 R.J. Levis, G.M. Menkir, H. Rabitz: *Science* **292**, 709 (2001)
- 9 Y.S. Cheng, E.B. Barr, B.J. Fan, P.J. Hargis, D.J. Rader, T.J. O'Hern, J.R. Torczynski, G.C. Tisone, B.L. Preppernau, S.A. Young, R.J. Radloff, S.L. Miller, J.M. Macher: *Aerosol Sci. Technol.* **30**, 186 (1999)
- 10 S.C. Hill, R.G. Pinnick, S. Niles, Y.L. Pan, S. Holler, R.K. Chang, J.R. Bottiger, B.T. Chen, C.S. Orr, G. Feather: *Field Anal. Chem. Technol.* **3**, 221 (1999)
- 11 G.W. Faris, R.A. Copland, K. Mortelmans, B.V. Bronk: *Appl. Opt.* **36**, 958 (1997)
- 12 M. Lippitz, W. Erker, H. Decker, K.E. van Holde, T. Basche: *Proc. Natl. Acad. Sci.* **99**, 2772 (2002)
- 13 A. Rehms, P. Callis: *Chem. Phys. Lett.* **208**, 276 (1993)
- 14 R.M. Measures: *Laser Remote Sensing, Fundamentals and Applications* (Wiley–Interscience, New York 1984)
- 15 B. Wattelier, C. Sauteret, J.-C. Chanteloup, A. Migus: *Opt. Lett.* **27**, 213 (2002)